*Aerosol and Air Quality Research*, 18: 749–761, 2018

ISSN: 1680-8584 print / 2071-1409 online
doi: 10.4209/aaqr.2017.12.0588

# PAH Profiles of Emitted Ashes from Indoor Biomass Burning across the Beijing-Tianjin-Hebei Region and Implications on Source Identification

**Zhiyong Li[1*], Lin Fan[1], Lei Wang[2], Huiqiao Ma[1], Yao Hu[1], Yunjun Jiang[2], Caixiu An[2], Aiqin Liu[2], Jinbao Han[3], Hui Jin[4]**

[1] *School of Environmental Science and Engineering, North China Electric Power University, Baoding, Hebei 071000, China*
[2] *Central Laboratory of Geology and Mineral Resources of Hebei Province, Baoding, Hebei 071003, China*
[3] *College of Quality and Technical Supervision, Hebei University, Baoding, Hebei 071002, China*
[4] *M&T Center of EHV Power Transmission Company of CSG, Guangzhou, Guangdong 510663, China*

## ABSTRACT

Sixty-four bottom ash (BA) samples from indoor burning of eight bio-fuels (BFs) including cotton (COT), corn (COR), millet (MIL), soybean (SOY), sorghum (SOR) and sesame (SES), firewood walnut (WAL), and corn cob (COC) were collected across the Beijing-Tianjin-Hebei (BTH) region. Each BA was divided into five differently sized parts for the analysis of eighteen PAHs using the GC/MS system. The $\Sigma_{18}$PAHs values for all the BAs varied from 65.0 ± 10.6 to 1310 ± 129 ng $g^{-1}$. SOR had the highest PAH level, and COC produced the lowest level. The $\Sigma_{18}$PAHs for SOY, WAL, COT, COR, COC, and SES were negatively correlated with the BA sizes. The NA, PHE, ACL, AN, FA, PY, FL, and AC dominated in all the BAs except for SES. All the BAs were dominated by 2, 3-ring PAHs. The PAH profiles for differently sized BAs within MIL, SOR, COC, COR, and SES were similar based on lower coefficient of divergence values, while the other three BFs did not exhibit this trend. All the BF pairs except for SOR vs. SES and COC vs. COR had the different PAH profiles. No series of coincident diagnostic ratios (DRs) could represent all BFs based on their significantly varied DRs. AN/(AN + PHE) and BA/BgP might be used in identification of combustion sources of different types of BFs. SOR and SES had higher potential toxicity risk based on higher TEQ, BaPE, and CPAHs values. BgF and BgP were the indicatory PAHs for SOY, MIL, COR, SOR, and COC, while they were AC and FL for the remaining three BFs.

***Keywords:*** Polycyclic aromatic hydrocarbon; Bottom ash; Bio-fuel; Diagnostic ratio; Indicatory PAHs.

## INTRODUCTION

The particle matter (PM) emitted from combustion of crop straws accounts for approximately 20% of the total PM amounts emitted from biomass burning around the world (Crutzen and Andreae, 1990; Streets *et al*., 2003). China as a large agricultural country. Its biomass utility as energy accounts for a large proportion of total energy consumption, especially in rural areas. China contributes approximately 25% of total biomass burning around Asia (Streets, *et al*., 2003), and biomass burned as energy accounts for 79.3% of total energy consumption in rural areas in China (Zhong *et al*., 2001). The improper use and waste of biomass resources not only results in serious atmospheric pollution, but also damages the ecological environment (Zhong *et al*., 2001; Hao *et al*., 2009).

Indoor air where working Zaotai stoves are located may contain various pollutants, such as CO, heavy metals, and PAHs. Also, some researchers have considered the emissions from Zaotai stoves for cooking and wood stoves for heating to be the major contributors to atmospheric pollution (Toscano *et al.*, 2014; Orecchio *et al*., 2016a). Serious atmospheric pollution incidents attributed to biomass burning have been frequently reported for domestic cities in Southeast Asia, India, Russia, and China (Permadi and Kim Oanh, 2013). Abas *et al*. (2004) reported that biomass combustion was the main source of organic aerosol during a heavy haze episode in Malaysia.

Polycyclic aromatic hydrocarbons (PAHs) are a class of typical persistent organic compounds originated from incomplete burning of coal, crop straws, garbage, and other organic substances (Liu *et al*., 2008; Masto *et al*., 2015; Li *et al*., 2016; Liu *et al*., 2016; Li *et al*., 2017a; Liu *et al*., 2017). When the incomplete combustion temperature is higher than 400°C, PAHs are often formed through aromatization reactions during the pyrolysis phase of BFs (Fisher *et al*.,

*Corresponding author.
Tel.: +86 312 7525506; Fax: +86 312 7525506
*E-mail address:* lzy6566@126.com

2002). The emitted PAHs from biomass burning have been a more focused issue, and their content varies significantly due to the compositional differences in types of BFs (Masto *et al*., 2015; Mahua, *et al*., 2017). Bottom ashes (BAs) can be used as soil conditioners due to their nutrient content (Ferreiro *et al*., 2011). However, the BAs from biomass burning can both adsorb and absorb large amounts of hazardous organic compounds (e.g., PAHs) and thus have adverse effects on human health (Košnář, *et al*., 2016).

Recently, BTH, as a culture and political center in north China, has been experiencing extreme, frequent atmospheric pollution episodes due to rapid urbanization and economic growth (Li *et al*., 2017; Zhang *et al*., 2017). Biomass burning is a main contributor of BTH atmospheric particles and PAHs. Indoor biomass burning contributes as much as 35–50% of BTH atmospheric particles (Li *et al*., 2017b). Inadequately treated bottom ashes (BAs) result in serious atmosphere and soil contamination. To our knowledge, few studies have been conducted on the characteristics of PAHs in BAs from BTH indoor biomass burning.

Therefore, systematic research on emitted PAHs in ashes for different BFs across BTH is necessary to comprehensively determine their utilization and assess their adverse environmental impacts. In this study, 64 BA samples were collected for 8 BFs across BTH. Each BA sample was divided into 5 differently sized parts, and a total of 320 BA samples were obtained for the analysis of 18 PAH congeners using the GC-MS system. The main aims of this study were to: 1) investigate the size distribution of total PAHs and individual PAH congeners for eight BFs, 2) compare the similarity of PAH profiles among ashes of different sizes within one BF and among different BFs in order to simplify the source apportionment of atmospheric PAHs, 3) assess the potential toxicity risk to human related to PAHs in ashes from indoor burning of 8 BFs, 4) analyze the diagnostic ratios of PAHs for the 8 BFs, and 5) identify the indicatory PAHs for the 8BFs.

## SAMPLE COLLECTION AND ANALYSIS

### *Sample Pre-treatment and Analysis*

The detailed sampling site distributions in BTH and the sampling project were documented in Li *et al*. (2017b). The BA samples were collected from Zaotai stoves across rural areas of BTH using a stainless steel shovel rinsed with n-hexane before sampling. All the BFs were fully dried in the sun before combustion, and the BA samples were dried using a vacuum dryer. We aimed at the same combustion conditions as those in actual cooking. The combustion started by igniting biomass with natural gas, and the BFs were burned down until the fire went out. The 8 samples for the 8 BFs were collected from each one of 8 sampling sites, and a total of 64 samples were obtained. A total of 2 kg of ash was collected using a pre-rinsed steel shovel and stored in a brown glass bottle. Then, each BA sample was divided into 5 differently sized parts using a vibrated screen, including 93–148 μm ($PM_{93–148}$), 67–93 μm ($PM_{67–93}$), 53–67 μm ($PM_{53–67}$), 40–53 μm ($PM_{40–53}$), and < 40 μm ($PM_{–40}$). Finally, the 320 BA samples were stored at –20°C before analysis.

The 18 PAHs were analyzed using the HP6890 GC/5973i MS for which the selected ion mode (SIM) was adopted. 18 PAHs were detected in this study, including naphthalene (NA), acenaphthylene (ACL), acenaphthene (AC), fluorine (Fl), benzo(g,h,i)perylene (BgP), phenanthrene (PHE), anthracene (AN), fluoranthene (FA), pyrene (PY), benzo(a)anthracene (BaA), chrysene (CHR), benzo(b)fluoranthene (BbF), benzo(k)fluoranthene (BkF), benzo(e)pyrene (BeP), benzo(a)pyrene (BaP), indeno(1,2,3-cd)pyrene (IP), dibenzo(a,h)anthracene (DBA), and coronene (COR).

The same sample pre-treatment and analysis method was adopted as that suggested in the EPA TO-13 and also adopted by Kong *et al*. (2011) and Li *et al*. (2016). The DB5-MS (length: 30 m; inner diameter: 0.25 mm; thickness: 0.25 mm) was used. The chromatographic conditions were as follows: 70°C held for 2 min, ramped to 260°C at 10 °C $min^{-1}$ and held for 8 min, then ramped to 300°C at 5 °C $min^{-1}$ and held for 5 min. Helium was used as the carrier gas at a constant flow of 1.0 mL $min^{-1}$. The detailed pre-treatment and analysis method can be reviewed in Kong *et al*. (2011) and is described simply as follows: 10 g of the BA sample was extracted with an ultrasonic wave using dichloromethane and was concentrated with a rotary evaporator. The extract was then purified in a gel column and concentrated again with a rotary evaporator. Finally, the volume was set at 0.5 mL by nitrogen blowing before analysis.

The m/z values used to distinguish PAH congeners were selected as 129, 127 for NA, 153, 152 for ACL, 151, 153 for AC, 165, 167 for Fl, 179, 176 for PHE and AN, 101, 203 for FA and PY, 229, 226 for BaA, 226, 229 for CHR, 256, 126 for BbF and BkF, 253, 126 for BaP and BeP, 138, 227 for IP, 139, 279 for DBA, 138, 227 for BgP, and 150, 301 for COR, respectively. Correspondingly, the quantitative m/z values were 128, 154, 152, 166, 178, 178, 202, 202, 228, 228, 252, 252, 252, 252, 276, 278, 276, 300 for NA, ACL, AC, FL, PHE, AN, FA, PY, BaA, CHR, BbF, BkF, BaP, BeP, IP, DBA, BgP, and COR, respectively.

### *Quality Control (QC) and Quality Assurance (QA)*

The entire pre-treatment and analysis procedure was strictly conducted according to the QC/QA programs. The sample blank, sample duplication, matrix spiked sample, and procedural blank experiments were conducted on schedule every 6 samples. The results indicated that no target chemicals were found in the solvent or procedural blank experiments.

The method detection limits (MDLs) (reported in ng $g^{-1}$) for the 18 PAHs were 1, 0.37, 0.40, 0.39, 0.12, 0.14, 0.14, 0.26, 0.19, 0.16, 0.14, 0.37, 0.32, 0.27, 0.30, 0.17, 0.17, and 0.30 for NA, ACL, AC, FL, BgP, IP, DBA, BbF, BkF, PHE, AN, FA, BaA, CHR, PY, BaP, BeP, and COR, with a mean value of 0.289 ± 0.202. The recovery rates for the 18 PAHs in 54 matrix added samples ranged from 78% to 119%. The surrogate standards, such as 14-deuterium substituted terphenyl and 4-bromo-2-fluorobiphenyl in 320 samples, had recoveries of 89 ± 12% and 92 ± 10%, respectively. The relative standard deviation (RSD) values for the 54 duplicated samples were all less than 10%.

## RESULTS AND DISCUSSION

### *Total Contents of 18 PAHs for All BFs*

Among the 8 BFs, the total content of the 18 PAHs ($\Sigma_{18}$PAHs) for 6 BFs (SOY, WAL, COT, COR, COC, and SES) were all negatively correlated with the particle sizes, while MIL and SOR didn't display this trend (Fig. 1). The $\Sigma_{18}$PAHs for all the BAs varied significantly from 65.0 ± 10.6 to 1310 ± 129 ng $g^{-1}$. The various sized BAs of SOR had the highest PAH levels (from 1100 ± 160 to 1310 ± 129 ng $g^{-1}$), while those from COC produced the lowest levels (65.0 ± 10.6 to 338 ± 68.9 ng $g^{-1}$). The highest TOC values for the different sized BAs from SOR among the 8 BFs were possibly the reason for this finding. The corresponding values (reported in ng $g^{-1}$) for the other 6 BFs ranged from 294 ± 55.6 to 1140 ± 191 for SOY, 651 ± 100 to 897 ± 102 for MIL, 90.3 ± 12.6 to 747 ± 110 for WAL, 358 ± 65.6 to 799 ± 118 for COT, 300 ± 41.1 to 469 ± 88.0 for COR, and 338 ± 66.8 to 576 ± 98.9 for SES, respectively. The TOC values were analyzed for 320 BA samples in order to assess the influence of incomplete combustion. The TOC values were corrected well with the Σ18PAHs values for all the BAs ($R^2$ = 0.89, P < 0.005), indicating incomplete combustion and suggesting that the BF species were important factors influencing the PAH emissions. Košnář *et al*. (2016) also reported the main factors contributing to PAH emission to be combustion temperature and BF species, while Masto *et al*. (2015) indicated that fuel species was less important than combustion conditions in PAH emissions.

Compared with the results of similar studies, the$\Sigma_{18}$PAHs (reported in ng $g^{-1}$) for all BFs in this study were much higher than 21.9 ($\Sigma_{18}$PAHs) for fly ashes (FAs) from 16 Chinese coal fired power plants (CFPPs) with individual block power capacity (IBPC) of 600 MW (Li *et al*., 2016) and 29.8–63.8 ($\Sigma_{16}$PAHs) for BAs from 48 biomass-fired power plants (BFPPs) in the Czech Republic (Zdeněk *et al*., 2016), much lower than 3466–4766 ($\Sigma_{16}$PAHs) for FAs from a Chinese CFPP with IBPC of 300 MW (Li *et al*., 2014), 3590–193,000 ($\Sigma_{16}$PAHs) for BAs from 4 Indian BFPPs (Masto *et al*., 2015), 3860–148,991 ($\Sigma_{16}$PAHs) for FAs from 48 BFPPs in the Czech Republic (Zdeněk *et al*., 2016), 1200–15900 for bottom ashes from combustion of municipal solid waste (MSW) (Peng *et al*., 2016a), 1970–3710 for bottom ashes from combustion of hydrothermally treated MSW (Peng *et al*, 2016b), and 135,40 for FAs from coal pressurized combustion (Zhou *et al*., 2009), while they were in the range of 31–2610 ($\Sigma_{16}$PAHs) for FAs from 4 Indian BFPPs. The significant difference of PAH levels among these studies were possibly resulted from the difference of fuel type, ash type, combustion conditions and the degree of burnout (Masto *et al*., 2015; Košnář *et al*., 2016; Li *et al*., 2016).

### *Content of Individual PAH Congeners in Different Sized BAs for 8 BFs*

Table 1 lists the mean content of individual PAHs for all five parts of the BAs from the 8 BFs. The 18 PAHs were all detected in BAs from 3 BFs (SOY, COT and SES), while only 10 out of the 18 PAHs were detected for COR and COC. The content of the 18 PAHs varied significantly among the different BFs. The mean content (reported in ng $g^{-1}$) of NA varied from 42.7 to 388 for all the BA samples, and those for PHE, ACL, AN, and FA were in the range of 5.51–255, 3.15–97.0, 0.567–75.9 and 1.00–121, respectively.

NA and PHE dominated in all the BAs. The other 6 top PAHs, including ACL, AN, FA, PY, FL, and AC, dominated in all the BA samples except for SES regardless of their highly variable content among the different BFs. In general, they were NA > PHE > FA > PY > AN > FL > ACL > AC, NA > PHE > ACL > FL > FA > PY > AC > AN, NA > PHE > FA > PY > ACL > AN > FL > AC, NA > PHE > FL > ACL > FA > AN > AC > PY, NA > PHE > FA > PY > FL > AN > ACL > AC, NA > PHE > FL > ACL > AC > FA > AN > PY, NA > PHE > FL > AC > ACL > FA > AN > PY for SOY, MIL, SOR, WAL, COT, COR, COC, and SES, respectively. However, the top PAHs in the BAs from SES followed FA > BbF > PY > AN > CHR. The PAHs

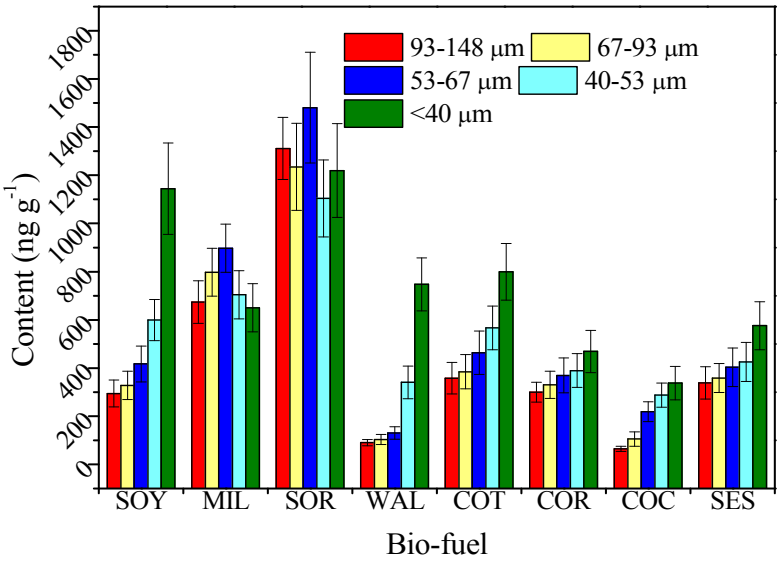


**Fig. 1.** Size distribution of total contents of 18 PAHs for 8 BFs.

**Table 1.** Mean content (ng $g^{-1}$) of individual PAH congener within different sized BAs from eight bio-fuels.

| BF | | NA | ACL | AC | FL | BgP | IP | DBA | BbF | COR | PHE | AN | FA | BaA | CHR | PY | BaP | BeP | BkF |
|---|---|---|---|---|---|---|---|---|---|---|---|---|---|---|---|---|---|---|---|
| SOY | *a* | 155 | 7.85 | 3.42 | 4.66 | 1.85 | 1.52 | nd | 4.01 | nd | 65.6 | 9.19 | 19.7 | 2.35 | 5.56 | 10.6 | 0.731 | 1.81 | 0.399 |
| | *b* | 168 | 8.26 | 3.73 | 4.67 | 1.88 | 1.58 | nd | 5.09 | nd | 73.8 | 10.8 | 22.9 | 2.52 | 8.12 | 12.3 | 0.979 | 2.36 | 0.677 |
| | *c* | 198 | 10.1 | 7.26 | 9.29 | 4.00 | 2.51 | 1.17 | 8.91 | nd | 93.3 | 14.1 | 30.0 | 4.59 | 10.7 | 16.9 | 1.73 | 3.52 | 0.899 |
| | *d* | 247 | 15.0 | 12.2 | 23.1 | 8.14 | 7.54 | 2.74 | 17.4 | 1.90 | 132 | 23.4 | 44.3 | 9.17 | 16.2 | 27.1 | 3.96 | 5.85 | 2.10 |
| | *e* | 388 | 27.6 | 25.0 | 63.7 | 21.2 | 20.8 | 6.66 | 43.0 | 2.72 | 255 | 51.7 | 92.6 | 25.2 | 32.8 | 58.5 | 11.0 | 13.2 | 5.68 |
| MIL | *a* | 298 | 63.6 | 34.7 | 44.3 | 2.73 | 3.30 | nd | 7.09 | nd | 121 | 20.9 | 32.0 | 5.83 | 9.76 | 23.5 | 2.55 | 3.04 | 0.959 |
| | *b* | 313 | 72.8 | 39.1 | 54.3 | 3.79 | 4.46 | nd | 10.9 | nd | 151 | 30.3 | 45.9 | 9.64 | 15.0 | 37.2 | 3.78 | 4.92 | 1.40 |
| | *c* | 275 | 85.6 | 39.7 | 61.4 | 8.03 | 6.58 | 3.15 | 20.5 | nd | 175 | 39.5 | 62.6 | 17.3 | 25.1 | 57.3 | 7.66 | 9.96 | 2.36 |
| | *d* | 228 | 62.7 | 30.7 | 49.5 | 3.81 | 3.12 | nd | 12.7 | nd | 152 | 32.1 | 48.7 | 11.2 | 16.9 | 41.1 | 4.58 | 5.64 | 1.46 |
| | *e* | 203 | 46.4 | 22.5 | 49.2 | 3.34 | 3.07 | nd | 11.4 | nd | 151 | 32.8 | 50.5 | 11.1 | 15.7 | 40.4 | 3.75 | 5.16 | 1.31 |
| SOR | *a* | 260 | 97.0 | 27.0 | 86.0 | 47.8 | 48.3 | 7.58 | 66.8 | nd | 191 | 71.2 | 103 | 46.2 | 61.8 | 115 | 36.8 | 33.0 | 12.6 |
| | *b* | 248 | 76.7 | 17.6 | 62.6 | 48.7 | 47.8 | 7.56 | 64.5 | nd | 173 | 65.8 | 98.6 | 51.1 | 66.6 | 114 | 41.9 | 35.9 | 14.5 |
| | *c* | 214 | 83.9 | 26.1 | 87.5 | 69.8 | 71.0 | 11.8 | 91.6 | nd | 206 | 75.9 | 121 | 66.3 | 88.1 | 143 | 56.5 | 47.2 | 20.9 |
| | *d* | 153 | 49.1 | 11.3 | 46.1 | 59.9 | 64.3 | 10.2 | 77.1 | nd | 140 | 50.7 | 91.6 | 58.0 | 73.2 | 110 | 51.6 | 39.1 | 18.4 |
| | *e* | 172 | 46.2 | 11.3 | 48.0 | 68.1 | 73.9 | 12.2 | 86.1 | nd | 145 | 53.2 | 96.9 | 67.2 | 86.0 | 122 | 61.2 | 47.9 | 22.6 |
| WAL | *a* | 45.9 | 4.23 | 4.62 | 8.43 | nd | nd | nd | nd | nd | 22.0 | 1.48 | 1.95 | 0.236 | 0.325 | 1.12 | nd | nd | nd |
| | *b* | 50.5 | 6.14 | 4.83 | 11.1 | nd | nd | nd | nd | nd | 24.2 | 1.78 | 2.58 | 0.256 | 0.361 | 1.28 | nd | nd | nd |
| | *c* | 62.2 | 9.57 | 7.20 | 12.7 | nd | nd | nd | nd | nd | 30.4 | 2.47 | 3.70 | 0.281 | 0.374 | 1.96 | nd | nd | nd |
| | *d* | 163 | 14.1 | 14.7 | 33.5 | 1.36 | nd | nd | 2.44 | nd | 73.3 | 6.84 | 15.5 | 2.00 | 2.62 | 8.86 | 0.565 | 1.01 | 0.537 |
| | *e* | 337 | 31.0 | 31.5 | 77.9 | 3.27 | 3.20 | nd | 10.4 | nd | 151 | 15.3 | 40.8 | 6.84 | 10.5 | 22.3 | 2.12 | 2.48 | 1.54 |
| COT | *a* | 145 | 15.2 | 8.34 | 15.4 | 3.00 | 3.52 | nd | 7.15 | nd | 79.6 | 13.8 | 30.4 | 4.40 | 8.29 | 19.8 | 0.925 | 2.36 | 0.621 |
| | *b* | 140 | 16.0 | 9.95 | 18.1 | 3.85 | 4.93 | nd | 10.0 | nd | 86.1 | 16.0 | 34.0 | 6.37 | 10.1 | 23.5 | 1.54 | 3.25 | 1.06 |
| | *c* | 157 | 16.6 | 9.97 | 23.1 | 8.42 | 9.25 | nd | 17.1 | nd | 98.3 | 19.2 | 43.0 | 9.51 | 12.9 | 28.6 | 3.56 | 5.02 | 1.79 |
| | *d* | 183 | 19.6 | 12.2 | 29.6 | 13.2 | 13.7 | 3.70 | 21.2 | 2.85 | 124 | 21.4 | 46.6 | 11.7 | 15.9 | 28.87 | 9.33 | 6.91 | 2.93 |
| | *e* | 221 | 20.1 | 12.5 | 33.0 | 36.8 | 38.6 | 3.75 | 49.6 | 12.2 | 131 | 28.5 | 61.9 | 24.0 | 29.1 | 45.5 | 25.7 | 17.4 | 8.78 |
| COR | *a* | 197 | 19.2 | 17.5 | 23.5 | nd | nd | nd | nd | nd | 30.8 | 4.17 | 4.32 | 0.408 | 0.465 | 2.14 | nd | nd | nd |
| | *b* | 198 | 25.0 | 22.9 | 32.7 | nd | nd | nd | nd | nd | 38.6 | 5.23 | 4.67 | 0.418 | 0.495 | 2.30 | nd | nd | nd |
| | *c* | 200 | 29.6 | 24.8 | 40.5 | nd | nd | nd | nd | nd | 55.3 | 7.81 | 6.87 | 0.561 | 0.596 | 3.57 | nd | nd | nd |
| | *d* | 202 | 29.8 | 24.9 | 43.8 | nd | nd | nd | nd | nd | 64.2 | 9.25 | 9.31 | 0.572 | 0.682 | 4.94 | nd | nd | nd |
| | *e* | 206 | 30.1 | 29.6 | 60.3 | nd | nd | nd | nd | nd | 98.5 | 14.6 | 17.5 | 1.02 | 1.32 | 9.57 | nd | nd | nd |
| COC | *a* | 42.7 | 3.15 | 4.89 | 5.76 | nd | nd | nd | nd | nd | 5.51 | 0.551 | 1.007 | 0.245 | 0.145 | 1.01 | nd | nd | nd |
| | *b* | 63.5 | 7.64 | 9.03 | 10.5 | nd | nd | nd | nd | nd | 10.8 | 0.567 | 1.20 | 0.378 | 0.228 | 1.51 | nd | nd | nd |
| | *c* | 119 | 13.9 | 13.3 | 23.0 | nd | nd | nd | nd | nd | 40.5 | 2.64 | 3.55 | 0.496 | 0.341 | 1.85 | nd | nd | nd |
| | *d* | 179 | 14.4 | 15.6 | 25.5 | nd | nd | nd | nd | nd | 39.4 | 4.21 | 5.34 | 1.27 | 0.799 | 2.16 | nd | nd | nd |
| | *e* | 204 | 17.1 | 20.2 | 29.1 | nd | nd | nd | nd | nd | 50.3 | 5.59 | 5.44 | 1.51 | 1.11 | 3.25 | nd | nd | nd |
| SES | *a* | 68.7 | 9.28 | 2.88 | 4.69 | 15.7 | 16.3 | 1.01 | 22.3 | 6.06 | 68.7 | 15.7 | 34.1 | 11.8 | 16.8 | 23.5 | 7.55 | 9.89 | 3.36 |
| | *b* | 70.9 | 9.32 | 3.00 | 5.40 | 17.9 | 16.4 | 1.22 | 24.0 | 6.49 | 70.8 | 16.8 | 37.1 | 12.9 | 18.1 | 25.0 | 8.83 | 10.8 | 4.03 |
| | *c* | 84.9 | 9.89 | 4.14 | 6.68 | 19.3 | 17.8 | 1.47 | 25.5 | 6.87 | 80.5 | 19.8 | 39.4 | 14.3 | 19.7 | 27.4 | 9.33 | 11.6 | 4.17 |
| | *d* | 95.0 | 10.5 | 3.49 | 7.41 | 20.2 | 20.0 | 1.59 | 26.7 | 8.15 | 81.1 | 19.9 | 40.9 | 15.1 | 20.8 | 28.1 | 9.96 | 12.2 | 4.68 |
| | *e* | 127 | 15.2 | 6.12 | 12.6 | 27.2 | 22.9 | 2.34 | 36.4 | 9.02 | 112 | 30.6 | 59.5 | 20.7 | 29.2 | 29.2 | 12.9 | 16.7 | 6.01 |

*a*: $PM_{93–148}$, *b*: $PM_{67–93}$, *c*: $PM_{53–67}$, *d*: $PM_{40–53}$ , *e*: $PM_{-40}$.
nd: not detected.

including COR, DBA, and IP had the lowest levels among all the BAs (Table 1).

Masto *et al*. (2005) suggested that the dominant PAHs were NA, PHE, BbF, and FA in BAs from a biomass (consisting of coconut, chicken and wood waste) fired power plant, while FAs dominated with NA, PHE, ACL, and PY in fly ashes. Zhou *et al*. (2009) reported the predominant PAHs to be CHR, FA and PHE, and NA, FA, and PHE in FAs from coal and residue char-pressured combustion, respectively. Liu *et al*. (2000) reported ACL, FA, and FL to be the top PAHs in FAs from fluidized bed combustion of coal at 800°C. Singh *et al*. (2003) reported that the top PAHs were AN, FA, BaA, and CHR for indoor BF combustion processes in rural areas in India. Li *et al*. (2014) reported them to be PHE, PY, NA, and FA in FAs from a Chinese coal fired power plant of 300 MW. Li *et al*. (2015) indicated them to be NA, ACL, and FA in the FAs from solid waste combustion in a rotary kiln incinerator. Li *et al*. (2016) reported them to be NA, PHE, FL, FA and CHR for FAs from Chinese coal-fired power plants (CFPPs) with individual power capacity of 600 MW, while they were NA, PHE, FA, PY and FL for CFPPs with lower individual power capacity ranging between 200 and 300 MW. Valavanidis *et al*. (2008) reported the PAH profiles for emitted soot particles from combustion of 6 types of common plastics. The predominant PAHs were NA, BkF, and AN for polystyrene,

NA, AN and CHR for poly vinyl chloride, NA, FL, and PHE for low density polyethylene, NA, PHE, and FL for high density polyethylene, and NA, AC, and FL for polypropylene and polyethyleneterephthalate, respectively. Orecchio *et al*. (2016a) reported the PAHs in the ashes of indoor combustion of wood pellets for heating in Italy and indicated that they were NA, PHE, and AN for burning of fir, NA, PHE, and FA for a mixture of fir and beech, and NA, PHE and ACL for conifers, respectively.

As the most toxic congener, BaP is the most carcinogenic (Kong *et al*., 2011). It should be noted that the highest content of BaP, in the range of 36.8–61.2 ng $g^{-1}$, was found in the BAs from SOR, indicating their strong toxicity.

The congener composition difference among different studies is a result of the choice of fuel species, the combustion conditions, and the particle size of the ashes (Košnář *et al*., 2016; Li *et al*., 2016). However, fuel species has been found to be the prevailing factor (Košnář *et al*., 2016).

***Potential Toxicity Risk Assessment***

Widely known parameters, including total carcinogenic PAHs (C-PAHs), BaP-based equivalent carcinogenic power (BaPE), BaP-based equivalency concentration (BaPeq), and 2,3,7,8-tetrachlorodibenzodioxin (TCDD)-based toxic equivalency concentration (TEQ), have been extensively applied to assessing PAH risks to humans (Kong *et al*., 2011; Cheruiyot *et al*., 2015; Li *et al*., 2016; Orecchio *et al*., 2016a). The calculated results of potential toxicity risk for the 8 BFs are listed in Table 2. The BaPeq (%) values of each PAH varied significantly among the 8 BFs as a result of their varied concentrations and BaP-based equivalent factors (Li *et al*., 2016). FA and BbF had higher BaPeq (%) values than the other PAHs, which is similar to those found for coal fired power plants with individual block power capacity ranging from 200 to 300 MW (Li *et al*., 2016). For the C-PAHs, SOR and SES produced the highest levels of 281–409 and 79.1–130 ng $g^{-1}$, while COR and COC had the lowest values. Similar results to those found for the C-PAHs were found for the TEQ concentrations. SOR and SES had the highest TEQ levels (64.5–101 and 12.0–20.3 ng $g^{-1}$). SOR, SES and COT had higher BaPE values compared with the other BFs. The BaPE of SOR (53.5–86.1 ng $g^{-1}$) was higher than those found for domestic burning of bituminous coal (Beijing and Shanxi, 30.5/60.6), anthracite coal (Beijing and Shanxi, 0.1/0.2), and honeycomb Briquette (Beijing and Shanxi, 1.1/42.7) in high heat mode (Liu *et al*., 2009). The BaPE values for SOY, MIL, COT, and SES were higher than those of anthracite coal (Beijing and Shanxi) and honeycomb briquette (Beijing) (Liu *et al*., 2009). The BaPE values for SOR, SOY, MIL, COT, and SES were significantly higher than that (0.570) of Chinese coal fired power plants with individual block power capacity of 600 MW (Li *et al*., 2016). Therefore, comprehensive utilization should be cautionary based on high potential toxicity risks.

**Table 2.** BaPeq and BaPE for eight BFs and BaPeq ratios for individual PAH congener.

| PAHs | TEF[b] | BaPeq[a] (%) | | | | | | | |
|---|---|---|---|---|---|---|---|---|---|
| | | SOY | MIL | SOR | WAL | COT | COR | COC | SES |
| PHE | 0.0005 | 1.16–4.49 | 1.14–2.37 | 0.118–0.260 | | 0.255–4.30 | --[f] | -- | 0.401–0.455 |
| AN | 0.0005 | 0.235–0.629 | 0.258–0.437 | 0.043–0.097 | | 0.055–0.746 | -- | -- | 0.095–0.119 |
| FA | 0.05 | 42.1–135 | 40.9–67.3 | 7.92–14.0 | | 12.0–137 | -- | -- | 21.0–23.1 |
| PY | 0.001 | 0.532–1.45 | 0.748–1.08 | 0.200–0.313 | 1.05–1.57 | 0.177–2.14 | -- | -- | 0.226–0.331 |
| **BaA** | 0.005 | 1.15–1.61 | 1.14–1.48 | 0.549–0.628 | 1.61–1.77 | 0.467–2.38 | -- | -- | 0.730–0.820 |
| **CHR** | 0.03 | 8.95–24.9 | 9.83–12.6 | 4.22–5.04 | 13.9–14.9 | 3.40–26.9 | -- | -- | 6.15–6.79 |
| **BbF** | 0.1 | 39.1–54.9 | 26.8–30.4 | 14.1–18.2 | 43.2–49.1 | 19.3–79.3 | -- | -- | 26.8–29.5 |
| **BkF** | 0.05 | 2.58–3.46 | 1.54–1.88 | 1.71–1.85 | 3.63–4.75 | 1.57–3.44 | -- | -- | 2.23–2.35 |
| **BaP** | 1.0 | 100 | 100 | 100 | 100 | 100 | 100 | 100 | 100 |
| **IP** | 0.1 | 14.5–20.8 | 6.81–12.9 | 11.4–13.1 | -- | 14.7–38.1 | -- | -- | 17.8–21.6 |
| **DBA** | 1.1 | nd–76.1 | nd–45.2 | 19.8–22.7 | -- | 16.1–43.6 | -- | -- | 14.7–20.0 |
| BgP | 0.02 | 3.85–5.06 | 1.66–2.14 | 2.23–2.60 | 3.08–4.81 | 2.83–6.49 | -- | -- | 4.05–4.22 |
| CPAHs[c] | | 14.6–145 | 29.4–82.7 | 281–409 | 0.561–34.6 | 24.9–180 | 0.873–2.34 | 0.390–2.62 | 79.1–130 |
| BaPE[d] | | 1.30–21.6 | 3.72–12.7 | 53.5–86.1 | 0.014–3.12 | 2.01–36.6 | 0.024–0.061 | 0.015–0.097 | 12.0–20.3 |
| TEQ[e] | | 1.99–29.1 | 5.22–17.0 | 64.5–101 | 0.130–5.30 | 3.06–43.0 | 0.381–0.713 | 0.100–0.547 | 14.6–25.1 |

[a] The BaP-based toxic equivalency factor (BaPeq) of individual PAH (i) is calculated as follows:

$$BaP_{eq,i}(\%) = \frac{PAH_{i,TEF} \times PAH_{i,EF}}{PAH_{BaP,TEF} \times PAH_{BaP,EF}}$$

[b] BaP-based toxicity equivalent factors (TEF) are referred to Liu *et al*. (2009).

[c] Sum of seven carcinogenic PAHs (marked by bold font) (ng $g^{-1}$).

[d] The BaP-equivalent carcinogenic power (BaPE) for the total PAHs (ng $g^{-1}$): BaPE = BaA × 0.06 + B[b,k]F × 0.07 + BaP + DBA × 0.6 + Ind × 0.08 (Liu *et al*., 2009; Li *et al*., 2016).

[e] TEQ: Total toxicity potency (TEQ) of the 16 PAHs is calculated by TEQ = $\Sigma PAH_i \times TEF_i$. TEF values are referred to Nisbet and LaGoy (1992) and as follows: NA 0.001; ACL 0.001; AC 0.001; FL 0.001; PHE 0.001; AN 0.01; FA 0.001; PY 0.001; BaA 0.1; CHR 0.01; BbF 0.1; BkF 0.1; BaP 1; IP 0.1; DBA 1; BgP 0.01.

[f] The absent value is resulted from not detectable BaP.

### *Composition Profiles of PAH Homologs with Different Rings for 8 BFs*

Fig. 2 lists the ring size distributions of the PAHs in the BAs from all BFs. The PAHs are often classified into three categories (low, medium, and high) according to their molecular weight, and are called LMW-, MMW, and HMW-PAHs, respectively (Kong *et al*., 2011; Li *et al*., 2016). The 2- and 3-ring compounds are contained in LMW-PAHs, 4-ring compounds belong to MMW-PAHs, and 5-, 6- and 7-ring compounds belong to HMW-PAHs. The BAs from all BFs were dominated by LMW-PAHs, especially the BAs from COR, COC, COT, and WAL. The HMW-PAHs were not detected in emitted BAs from COR and COC. The LMW-PAHs contributed 78.3 ± 5.16%, 80.2 ± 4.43%, 46.9 ± 7.20%, 92.5 ± 4.39%, 69.3 ± 8.31%, 96.4 ± 1.61%, 96.7 ± 0.311%, and 50.8 ± 1.34 to the total PAH concentrations of SOY, MIL, SOR, WAL, COT, COR, COC, and SES, respectively. Similar results have been reported elsewhere. SOR and SES had the highest ratios among the MMW-PAHs of 28.1 ± 2.36% and 25.0 ± 0.721%, respectively. The lowest ratios for MMW-PAHs of 3.28 ± 0.311% and 3.65 ± 1.61%, respectively, occurred in the BAs from COC and COR. The LMW-PAHs varied significantly from reported values found elsewhere, where they contributed 42.54% and 41.4% to the total PAHs in fly ashes originating from the combustion of coal and residual char in a pressurized spouted fluidized bed (Zhou *et al*., 2009), 86.9 ± 13.0% and 47.9 ± 26.2% of total PAHs in fly ashes and bottom ashes, respectively, from four Indian biomass fired power plants (Masto *et al*., 2015), and where 32.7% and 44.5% of total PAHs were attributed to LMW-PAHs for bottom ashes from a sample of phytomass and dendromass -fueled power plants in the Czech Republic (Košnář *et al*., 2016).

### *Similarity Comparison of PAH Profiles among Different BFs and Different Sized BAs within One BF*

A widely known parameter coefficient of divergence (a self-normalizing parameter) has been extensively used to distinguish the PAH profiles between two sources and can be calculated as follows (Kong *et al*., 2011; Li *et al*., 2016, 2017b):

$$CD_{jk} = \sqrt{\frac{1}{p}\sum_{i=1}^{p}\left(\frac{X_{ij} - X_{ik}}{X_{ij} + X_{ik}}\right)^2}\ , \qquad (1)$$

where $CD_{jk}$ refers to the PAH profiles for two different BFs or two different sized ashes for one BF; p is number of analyzed PAH congeners for each ash, and $x_{ij}$ and $x_{ik}$ are the normalized concentrations of PAH i for j and k (Wongphatarakul *et al*., 1998; Kong *et al*., 2011; Li *et al*., 2016, 2017b). The PAH profiles between the two emission sources were similar in that the CD value approach zero and was different if CD approached one (Wongphatarakul *et al*., 1998). Both Kong *et al*. (2011) and Li *et al*. (2016, 2017b) used 0.3 as the threshold value to identify the similarity of source profiles.

Table 3 lists the mean values between any two different sized BAs for each BF. Among the different sized BAs within one BF, the PAH profiles (PAHPs) between two neighboring BAs were more similar than those of two separated ones based on the lower CD values of neighboring BAs. For example, the CD values of the neighboring $PM_{93–148}$ vs. $PM_{67–93}$ for all BFs were lowest compared with those of $PM_{93–148}$ vs. $PM_{53–67}$, $PM_{93–148}$ vs. $PM_{40–53}$ and $PM_{93–148}$ vs. $PM_{–40}$. Also the CD values of $PM_{67–93}$ vs. $PM_{53–67}$ for all BFs were lower than $PM_{67–93}$ vs. $PM_{40–53}$ and $PM_{67–93}$ vs. $PM_{–40}$.

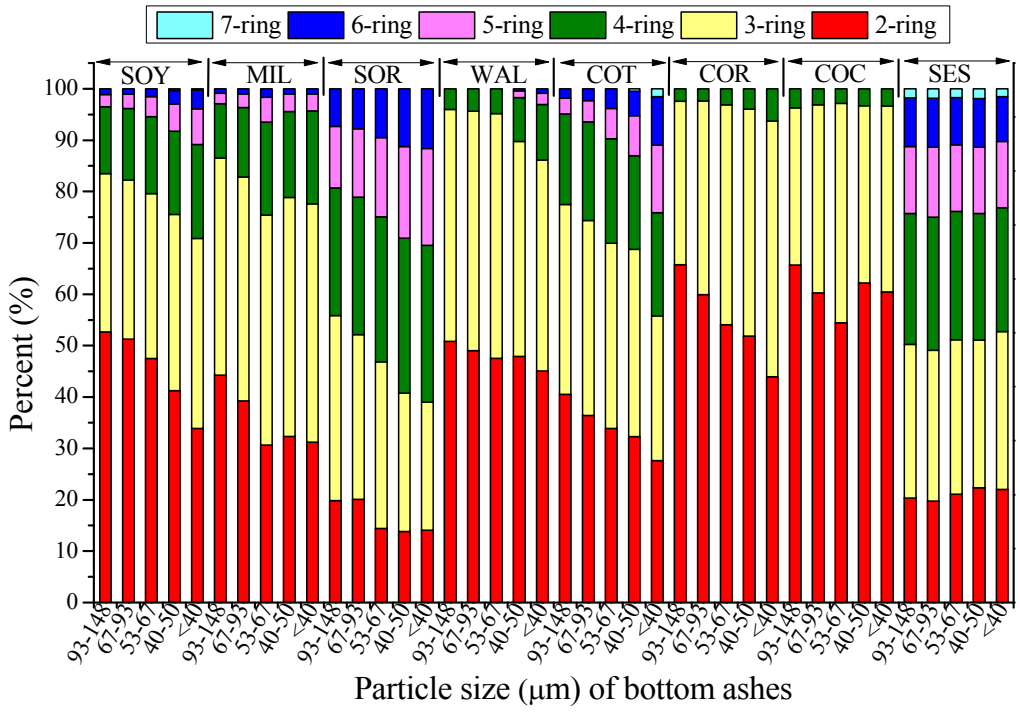


**Fig. 2.** Composition of ring sized PAHs in different sized BAs for 8 BFs.

**Table 3.** Mean CD value between any two differently sized BAs within the same BF.

| BF | a vs. b | a vs. c | a vs. d | a vs. e | b vs. c | b vs. d | b vs. e | c vs. d | c vs. e | d vs. e |
|---|---|---|---|---|---|---|---|---|---|---|
| SOY | 0.065 | 0.264 | **0.428** | **0.489** | 0.265 | **0.416** | **0.476** | 0.286 | **0.355** | 0.122 |
| MIL | 0.094 | 0.147 | 0.182 | 0.199 | 0.092 | 0.097 | 0.117 | 0.260 | 0.266 | 0.048 |
| SOR | 0.073 | 0.112 | 0.193 | 0.222 | 0.078 | 0.124 | 0.161 | 0.098 | 0.128 | 0.036 |
| WAL | 0.060 | 0.164 | **0.558** | **0.629** | 0.193 | **0.571** | **0.640** | **0.555** | **0.623** | 0.273 |
| COT | 0.103 | 0.220 | **0.438** | **0.533** | 0.136 | **0.396** | **0.543** | **0.349** | **0.428** | 0.238 |
| COR | 0.048 | 0.098 | 0.134 | 0.227 | 0.073 | 0.116 | 0.217 | 0.049 | 0.157 | 0.117 |
| COC | 0.086 | 0.127 | 0.128 | 0.148 | 0.156 | 0.164 | 0.167 | 0.117 | 0.129 | 0.046 |
| SES | 0.033 | 0.049 | 0.047 | 0.075 | 0.035 | 0.047 | 0.070 | 0.047 | 0.054 | 0.047 |

a: $PM_{93–148}$, b: $PM_{67–93}$, c: $PM_{53–67}$, d: $PM_{40–53}$, e: $PM_{–40}$.
The bold numbers were higher than 0.3.

The PAHPs between any BA pairs in MIL, SOR, COC, COR, and SES were all similar based on their having CD values lower than 0.3, which implied the PAHPs of different sized BAs from these 5 BFs can replace each other. However, for SOY, WAL, and COT, only partially paired BAs had CD values less than 0.3, indicating that the PAHPs for the different sized BAs in these BFs could not replace each other.

Due to the similarity of the PAHPs among the different sized BAs in MIL, SOR, COC, COR, and SES, those of $PM_{53–67}$ were selected to represent these five BFs. The CD values for MIL vs. SOR, MIL vs. COC, MIL vs. COR, MIL vs. SES, SOR vs. COC, SOR vs. COR, SOR vs. SES, COC vs. COR, COC vs. SES and COR vs. SES were 0.413 ± 0.014, 0.704 ± 0.108, 0.735 ± 0.126, 0.489 ± 0.095, 0.781 ± 0.125, 0.775 ± 0.126, 0.223 ± 0.056, 0.091 ± 0.016, 0.802 ± 0.214, and 0.799 ± 0.136, respectively. The PAHPs of SOR vs. SES and COC vs. COR were similar based on their having CD values lower than 0.3.

For the remaining 3 BFs (including SOY, WAL, and COT) with different PAH profiles among the different sized BAs, the CD values were calculated for every BA pair between two BFs. The PAHPs for the two BFs were identified as being different if the CD value of any one pair of BAs was higher than 0.3. The results showed that the PAHPs for SOY, WAL, and COT were different from each other (Fig. 3).

***PAH Diagnostic Ratios***

The diagnostic ratios (DRs) of PAHs are always selected to identify the emission sources and have been effectively used in source apportionment of atmospheric PAHs (Kong *et al*., 2011; Li *et al*., 2016; Orecchio *et al*., 2016a, b). The detailed application of DRs in source apportionment has been described elsewhere (Ravindra *et al*., 2008; Tobiszewski and Namiesnik, 2012). Although the PAHPs for different emission sources are always different each other, the PAHPs are often replaced by DRs in source apportionment to eliminate the influence of chemical reactions with other pollutants (Li *et al*., 2016). The 5 BFs with the same PAHPs for the different sized BAs had similar DRs among all their BAs. The PAH DRs that have been frequently documented elsewhere were calculated for the finest BAs in that 8 BFs, as listed in Table 3. In this study, the DRs for every bio-fuel refers to the weighed mean according to the ash yield for different sized particles and can be calculated as follows:

$$DR_{BF} = \sum_{i=a}^{e} A_i \times DR_i \ , \quad (2)$$

where $DR_{BF}$ is the DR value for one type of BFs, and $A_i$ and $DR_i$ are the contribution rate (%) and diagnostic ratio of ash of a specific size, respectively. The $A_i$ values for seven BFs were reported by Li *et al*. (2017b).

The DRs documented elsewhere were calculated based on their reported PAH congener data. The DRs extensively used to identify the PAH origins for the eight BFs involved in this study and other industrial and domestic burning sources reported elsewhere are listed in Table 4.

Most ratios AN/(AN + PHE), BA/(BA + CHR), BA/CHR, BbF/BkF, BA/BgP, PY/BaP, and BA/BaP varied significantly among the 8 BFs, which indicated the strong influence of BF types on emitted PAHs and suggested that no series of coincident DRs can represent all BFs (Table 4). BA/CHR and BbF/BkF could be used to identify the combustion sources among four types of plastics (Budzinski *et al*., 1999; Lohmann e*t al*., 2000). COC had the highest BA/(BA + CHR) value among the 8 BFs. The BbF/BkF values of the Chinese BFs were significantly higher than those of the Indian biomasses. The lack of any detectable BkF in COR, COC, and WAL resulted in their absent BbF/BkF values. The ratio of BaP/COR for SES was 0.966, which was significantly lower than that for Chinese coal combustion for heating and power generation. The ratios of BaP/COR were not available for the other 7 BFs due to a lack of detectable COR or BaP.

BbF/BkF might be used to discriminate between BFs from domestic and industrial combustion sources. The ratios of AN/(AN + PHE) and BA/BgP might be used for identification of combustion sources of different types of BFs.

Of the two structural isomers, PHE has higher thermal stability than AN, so PHE enriched at low temperatures, and AN is often related to combustion processes (Orecchio *et al*., 2016b). The ratios of AN/(AN + PHE) in this study ranged from 0.068 to 0.271, with a mean value of 0.147, which indicated the association with combustion. AN/(AN + PHE) < 0.1 suggested low temperature sources (e.g., petroleum), while > 0.1 was an indication of the combustion sources (Toscano *et al*., 2014; Orecchio *et al*., 2016a, b). The ratios of FA/((FA + PY) in this study ranged from 0.462 for SOR to 0.662 for COR with mean values of 0.592 and higher than 0.5, respectively. The ratio of FA/(FA + PY) > 0.5 always

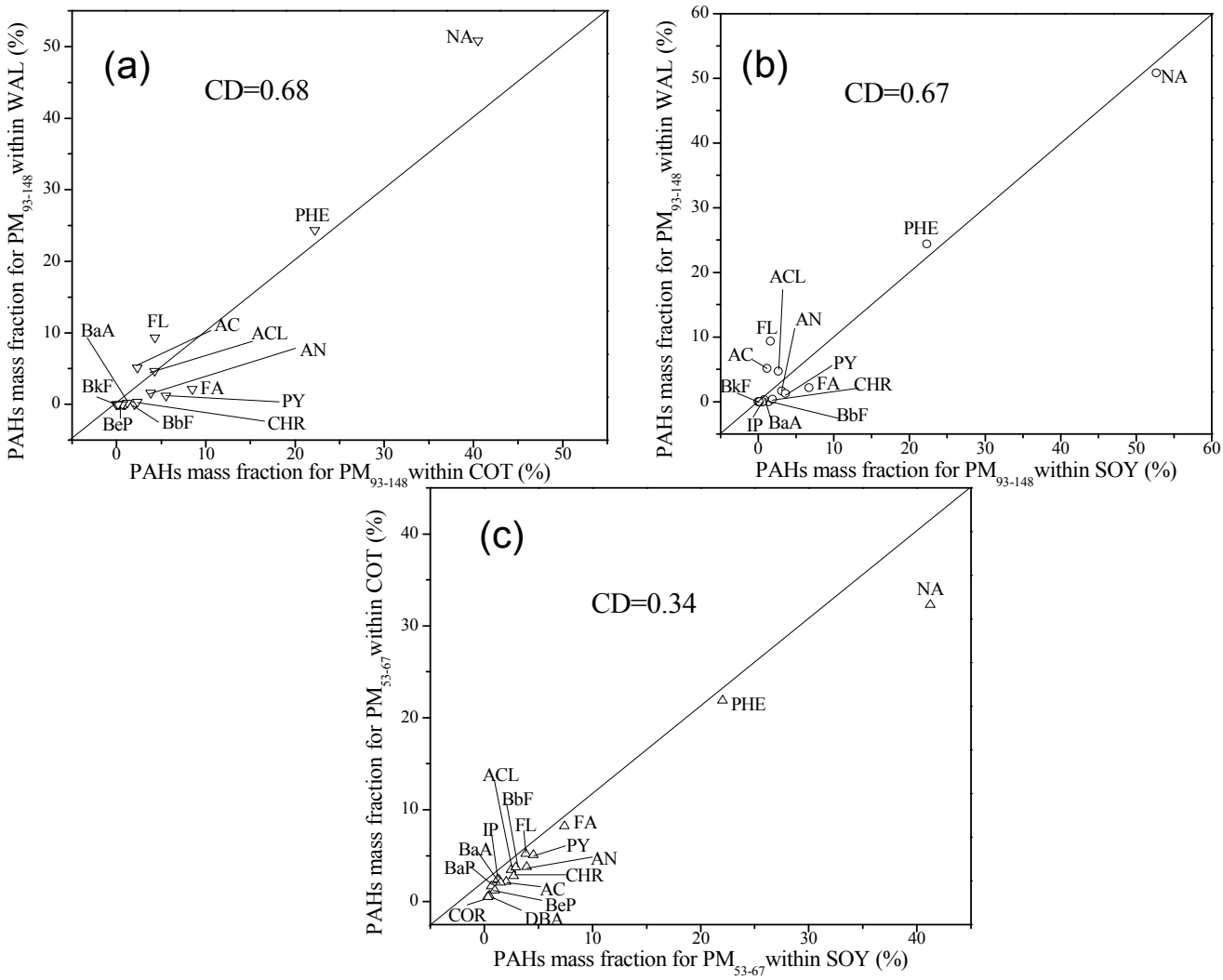


**Fig. 3.** Calculated CD for PAH profiles of a) $PM_{93–148}$ from WAL and COT, b) $PM_{93–148}$ from WAL and SOY and c) $PM_{53–67}$ from COT and SOY.

indicates the combustion of grass, wood, and coal, while a ratio of < 0.5 is an indication of petroleum or liquid fossil fuel combustion (Orecchio *et al*., 2016b). However, some combustion sources have been documented elsewhere, such as indoor burning of wood pellets for heating in Italy (Orecchio *et al*., 2016a), burning of crop residues for a power plant in the Czech Republic (Košnář *et al*., 2016), and indoor burning of fuelwood for cooking in India (Singh *et al*., 2013), with FA/(FA + PY) ratios lower than 0.5. A ratio of BA/(BA + CHR) > 0.35 implies combustion sources, 0.20–0.35 is related to petroleum or combustion sources, and a ratio < 0.20 indicates low temperature sources. In this study, the ratios of BA/(BA + CHR) ranged from 0.282 to 0.613 with higher mean value 0.426 as compared to 0.35, which implied the combustion sources. A ratio of IP/(IP + BgP) > 0.5 most likely implies that the combustion of grass, wood, and coal, in a range of 0.20–0.50, is related to liquid fossil fuel combustion, and where a ratio < 0.20 indicates a petroleum origin (Orecchio *et al*., 2016b). The ratios of IP/(IP + BgP) in this study were in the range of 0.450–0.510, with a lower mean value as 0.493 as compared to 0.50, which was in disagreement with the findings of Orecchio *et al*. (2016b). In some cases, the different DRs provided conflicting results in judgment of atmospheric sources (Orecchio, 2010a, b, c). The total index was calculated as shown in Eq. (3) to identify the pollution sources.

$$Total-index=\frac{FA/(FA+PY)}{0.4}+\frac{AN/(AN+PHE)}{0.2}+\frac{BA/(BA+CHR)}{0.1}+\frac{IP/(IP+BgP)}{0.5} \quad (3)$$

If the total index is higher than 4, this is an indication of high temperature sources as combustion, while it is related to low temperature sources if the value is lower than 4 (Orecchio *et al*., 2016b). The total index values for 8 BFs were all higher than 4, indicating they are associated with the combustion source.

***Indicatory PAHs for Each Type of Ash***

The indicatory PAHs, also known as source markers,

**Table 4.** Diagnostic ratios of several PAHs from some domestic and industrial combustion sources.

| Reference | | AN/ AN + PHE | FA/ FA +PY | BA/ BA+ CHR | BA/CHR | BbF/BkF | IP/BgP | IP/ IP + BgP | BA/BgP | BaP/COR | PY/BaP | BA/BaP | BaP/ BaP + CHR | Total Index |
|---|---|---|---|---|---|---|---|---|---|---|---|---|---|---|
| This study | MIL | 0.165 | 0.555 | 0.392 | 0.645 | 8.02 | 1.06 | 0.510 | 2.51 | -- | 9.31 | 2.46 | 0.208 | 7.15 |
| | SOR | 0.271 | 0.462 | 0.433 | 0.763 | 4.61 | 1.02 | 0.505 | 0.989 | -- | 2.67 | 1.20 | 0.389 | 7.85 |
| | COR | 0.122 | 0.662 | 0.462 | 0.860 | -- | -- | -- | -- | -- | -- | -- | -- | -- |
| | COC | 0.086 | 0.556 | 0.613 | 1.59 | -- | -- | -- | -- | -- | -- | -- | -- | -- |
| | SES | 0.193 | 0.600 | 0.416 | 0.712 | 6.21 | 0.969 | 0.492 | 0.743 | 0.966 | 2.90 | 1.53 | 0.318 | 7.61 |
| | SOY | 0.128 | 0.647 | 0.282 | 0.398 | 8.99 | 0.820 | 0.450 | 1.27 | -- | 12.8 | 2.87 | 0.122 | 5.98 |
| | COT | 0.156 | 0.599 | 0.395 | 0.659 | 9.16 | 1.05 | 0.508 | 1.26 | -- | 12.2 | 3.19 | 0.221 | 7.24 |
| | WAL | 0.088 | 0.656 | 0.418 | 0.718 | -- | -- | -- | -- | -- | -- | -- | -- | -- |
| [a]Plastic | PS | 0.569 | -- | 0.654 | 1.89 | 0.403 | -- | -- | -- | -- | -- | 0.515 | 0.617 | -- |
| | PVC | 0.598 | -- | 0.462 | 0.859 | 1.82 | -- | -- | -- | -- | -- | 0.614 | 0.609 | -- |
| | PP | 0.480 | -- | 0.379 | 0.657 | 0.636 | -- | -- | -- | -- | -- | 0.633 | 0.556 | -- |
| | PE | 0.406 | -- | 0.541 | 1.18 | 0.877 | -- | -- | -- | -- | -- | 0.61 9 | 0.664 | -- |
| [b]Heating | Fir | 0.471 | 0.190 | -- | -- | -- | -- | -- | -- | -- | 4.00 | -- | -- | -- |
| | Beech | 0.481 | 0.360 | -- | -- | -- | -- | -- | -- | -- | 0.500 | -- | -- | -- |
| [c]Cooking | FW[*] | 0.620 | 0.450 | 0.769 | 3.34 | 1.22 | -- | -- | -- | -- | 4.42 | 3.02 | 0.416 | -- |
| | DC[#] | 0.708 | 0.533 | 0.406 | 0.684 | 1.07 | 0.877 | 0.467 | 1.39 | -- | 1.12 | 1.56 | 0.305 | 9.87 |
| | CR[***] | 0.655 | 0.569 | 0.683 | 2.15 | -- | -- | -- | -- | -- | 4.82 | 4.03 | 0.453 | -- |
| [d]Power plant | Wood | 0.283 | 0.531 | 0.364 | 0.571 | 2.43 | 1.00 | 0.500 | 0.571 | -- | 0.852 | 0.593 | 0.491 | 7.38 |
| | Straw | 0.167 | 0.438 | 0.752 | 3.03 | 2.43 | 0.717 | 0.418 | 1.83 | -- | 2.19 | 1.65 | 0.628 | 10.3 |
| [e]Heating station (coal) | | 0.580 | 0.580 | 0.540 | 1.29 | 1.57 | 1.63 | 0.620 | 1.13 | 3.15 | 2.04 | 0.71 | 0.44 | 11.0 |
| [e]Coke | | 0.580 | 0.580 | 0.420 | 0.740 | 2.17 | 1.77 | 0.640 | 1.18 | 3.42 | 1.55 | 1.66 | 0.51 | 9.83 |
| [f]Power plant (Coal) | | 0.140 | 0.690 | 0.330 | 0.530 | 6.56 | 1.34 | 0.530 | 2.46 | 1.96 | 3.96 | 2.46 | 0.330 | 6.79 |
| [g]MSW[**]/coal | | 0.114 | 0.523 | 0.564 | 1.30 | 0.935 | -- | -- | -- | -- | 6.81 | 1.68 | 0.436 | -- |

[a] Valavanidis *et al*., 2008; [b] Orecchio *et al*., 2016; [c] Singh *et al*., 2013; [d] Košnář *et al*., 2016; [e] Kong *et al*., 2011; [f] Li *et al*., 2016; [g] You *et al*., 2002.
[*] Fuelwood; [#] Dung cake; [##] Crop residue; [**] Municipal solid waste.

tracers, indicators, or signatures may be used in the source apportionment of atmospheric PAHs (Kong *et al*., 2011). The identification of indicatory PAHs used in the chemical mass balance (CMB) model is the first step for assessing source contributions to ambient PAHs. Dominance of PAHs in emission sources is not the selection standard of indicatory PAHs for these sources (Ravindra *et al*., 2008). A formula shown here as Eq. (4) and recommended by Yang *et al*. (2002) has been extensively used to define indicatory PAHs.

$$Ratio_{j,i} = \frac{\left(X_i/\sum X\right)}{\left(X_i/\sum X\right)_{\min}}, \quad (4)$$

where $X_i$ is concentration of the ith individual PAH congener; $(X_i/\Sigma X)_j$ is the contribution of the ith individual PAH to the total PAHs in source j, and $(X_i/\Sigma X)_{min}$ is the minimum contribution value of the ith individual PAH to the total PAHs within all sources (Chen *et al*., 2003; Kong *et al*., 2011).

The two or three PAHs with the highest ratio values are identified as indicatory PAHs (Yang *et al*., 2002; Chen *et al*., 2003; Kong *et al*., 2011). NA is excluded from analysis because it is not defined as a PAH in a stricter sense, it is more like a volatile organic compound (VOC) due to its bicyclic structure (Kong *et al*., 2011).

Table 5 lists the indicatory PAHs for different sized ashes for the 8 BFs and for ashes from some other industrial stacks. Generally, the indicatory PAH profiles among different sized ashes for the same BFs were similar regardless of slight differences. Class I, including 5 BFs (SOY, MIL, SOR, SES, and COT) had similar indicatory PAH profiles, while Class II including 3 BFs (COR, COC, and WAL) had similar profiles. The 8 BFs were divided into two classes based on indicatory PAHs. BgP and BbF were the indicatory PAHs for Class I, while AC and FL were the indicatory PAHs for Class II. For Class I, the rings of indicatory PAHs were 5 and 6, while they were 3 for Class II. The significant difference between classes I and II were possibly a result of the differences in the chemical composition of the BFs and combustion temperatures (Kong *et al*., 2011; Li *et al*., 2016). It should be noted that different indicatory PAH profiles were found among different BFs, so we could not simply identify all the straws and wood pellets as one type of biomass in the source apportionment of the PAHs.

The indicatory PAHs for 8BFs were significantly different from those of other industrial stacks (Yang *et al*., 1998; Tsai, *et al*., 2007; Ravindra *et al*., 2008; Kong *et al*., 2011). Tsai *et al*. (2007) reported the indicatory PAH to be ACL for the coking industry, while Kong *et al*. (2011) reported it to be ACL, FL and AN for the same industry. Other PAH combinations have also been identified as marks for some industrial stacks in some previous studies. The PAH marks were found to be BaP and COR for the steel industry (Yang *et al*., 1998), ACL, AC and AN for the cement industry

**Table 5.** Indicatory PAHs for eight bio-fuels and other industrial stacks.

| Emission source | | Indicatory PAHs | Rings | Reference | Emission source | | Indicatory PAHs | Rings | Reference |
|---|---|---|---|---|---|---|---|---|---|
| SOY | $PM_{93–148}$ | BbF, BgP, IP | 5, 6 | This study | COR | $PM_{93–148}$ | AC, FL, ACL | 3 | This study |
| | $PM_{67–93}$ | BbF, BgP, BeP | 5, 6 | This study | | $PM_{67–93}$ | AC, FL, ACL | 3 | This study |
| | $PM_{53–67}$ | BbF, BgP, BeP | 5, 6 | This study | | $PM_{53–67}$ | AC, FL, ACL | 3 | This study |
| | $PM_{40–53}$ | BbF, BgP, IP | 5, 6 | This study | | $PM_{40–53}$ | AC, FL, ACL | 3 | This study |
| | $PM_{–40}$ | BbF, BgP, IP | 5, 6 | This study | | $PM_{–40}$ | AC, FL, ACL | 3 | This study |
| MIL | $PM_{93–148}$ | BbF, BgP, IP | 5, 6 | This study | COC | $PM_{93–148}$ | AC, FL, ACL | 3 | This study |
| | $PM_{67–93}$ | BbF, IP, BgP | 5, 6 | This study | | $PM_{67–93}$ | AC, FL, ACL | 3 | This study |
| | $PM_{53–67}$ | BbF, BgP, BeP | 5, 6 | This study | | $PM_{53–67}$ | AC, FL, ACL | 3 | This study |
| | $PM_{40–53}$ | BbF, BeP, BgP | 5, 6 | This study | | $PM_{40–53}$ | AC, FL, ACL | 3 | This study |
| | $PM_{–40}$ | BbF, BeP, BgP | 5, 6 | This study | | $PM_{–40}$ | AC, FL, ACL | 3 | This study |
| SOR | $PM_{93–148}$ | BgP, IP, BbF | 5, 6 | This study | SES | $PM_{93–148}$ | BgP, IP, BbF | 5, 6 | This study |
| | $PM_{67–93}$ | BgP, IP, BbF | 5, 6 | This study | | $PM_{67–93}$ | BgP, IP, BbF | 5, 6 | This study |
| | $PM_{53–67}$ | BgP, IP, BbF | 5, 6 | This study | | $PM_{53–67}$ | BgP, IP, BbF | 5, 6 | This study |
| | $PM_{40–53}$ | BgP, IP, BaP | 5, 6 | This study | | $PM_{40–53}$ | BgP, IP, BbF | 5, 6 | This study |
| | $PM_{–40}$ | BgP, IP, BaP | 5, 6 | This study | | $PM_{–40}$ | BgP, IP, BbF | 5, 6 | This study |
| WAL | $PM_{93–148}$ | FL, AC, PHE | 3 | This study | COT | $PM_{93–148}$ | BbF, IP, BgP | 5, 6 | This study |
| | $PM_{67–93}$ | FL, AC, ACL | 3 | This study | | $PM_{67–93}$ | BbF, IP, BgP | 5, 6 | This study |
| | $PM_{53–67}$ | FL, AC, ACL | 3 | This study | | $PM_{53–67}$ | BgP, IP, BbF | 5, 6 | This study |
| | $PM_{40–53}$ | FL, AC, PHE | 3 | This study | | $PM_{40–53}$ | BgP, IP, BbF | 5, 6 | This study |
| | $PM_{–40}$ | FL, AC, BaA | 3, 4 | This study | | $PM_{–40}$ | BgP, IP, BbF | 5, 6 | This study |

| Emission source | Indicatory PAHs | Rings | Reference |
|---|---|---|---|
| Steel industry | BaP, COR | 5, 7 | Yang *et al*. (1998) |
| Coke making plant | ACL | 3 | Tsai *et al*. (2007) |
| Cement industry | ACL, AC, AN | 3 | Ravindra *et al*. (2008) |
| Coke making plant | ACL, FL, AN | 3 | Kong *et al*. (2011) |
| Heating station (coal) | ACL, FL, AN | 3 | Kong *et al*. (2011) |
| Iron smelting plant | CHR, BbF, DBA | 4, 5 | Kong *et al*. (2011) |

(Ravindra *et al*., 2008), and CHR, BbF, and DBA for an iron smelting plant (Kong *et al*., 2011). The application of the indicatory PAH method in source apportionment should therefore be used with caution due to the significant influence of feed fuel, combustion temperature and device, combustion parameters, and types of air pollution control.

## CONCLUSIONS

The 320 different sized BAs (5 size ranges for each type of BF) were collected for 8 BFs from 8 sampling sites across the Beijing-Tianjin-Hebei region. The $\Sigma_{18}$PAHs values for all the BAs varied significantly from 65.0 ± 10.6 to 1310 ± 129 ng $g^{-1}$. SOR had the highest level, and COC had the lowest level. The $\Sigma_{18}$PAHs for 6 BFs including SOY, WAL, COT, COR, COC, and SES were all negatively correlated with the particle size of the BAs, while those for MIL and SOR didn't display this trend. The BAs from all BFs were dominated by LMW-PAHs, especially the BAs from COR, COC, COT, and WAL. The PAH profiles for the different sized BAs within MIL, SOR, COC, COR, and SES were similar based on lower CD values, while the other 3 BFs did not show this trend. NA and PHE dominated in all the BAs. The other 6 top PAHs (ACL, AN, FA, PY, FL, and AC) dominated in all the BA samples except for SES. SOR and SES had higher BaPE, TEQ and CPAHs levels compared with the other BFs. Generally, the BaPE for 5 of the 8 BFs in this study were higher than those for domestic combustion of coal in high heat mode. The ratios of AN/(AN + PHE), BA/(BA + CHR), BA/CHR, BbF/BkF, BA/BgP, PY/BaP, and BA/BaP varied significantly among the 8 BFs, which indicated the strong influence of BF type and implied that no series of coincident DRs can represent all BFs. The BbF/BkF ratio may be used to discriminate between domestic and industrial combustion sources for BFs and coal. The ratios of AN/(AN + PHE) and BA/BgP could be used in identification of combustion sources of different types of BFs. The indicatory PAHs for 8 BFs were significantly different from those of other industrial stacks. They were BbF and BgP for SOY, MIL, COR, SOR and COC, and were AC and FL for WAL, COT, and SES.

## ACKNOWLEDGEMENTS

This study was supported by the Fundamental Research Funds for the Central Universities (2017MS142), the National Natural Science Foundation of China (21407048) and the Scientific Research Foundation of the Higher Education Institutions of Hebei Province, China (QN2016024).

## REFERENCES

Abas, M.R.B., Rahman, N.A., Omar, N.Y.M.J., Maah, M.J., Samah, A.A., Oros, D.R., Otto, A. and Simoneit, B.R.T. (2004). Organic composition of aerosol particulate matter during a haze episode in Kuala Lumpur, Malaysia. *Atmos. Environ.* 38: 4223–4241.

Budzinski, H., Letellier, M., Garrigues, P. and Le Menach. K. (1999). Optimisation of the microwave-assisted extraction in open cell of polycyclic aromatic hydrocarbons from soils and sediments: Study of moisture effect. *J. Chromatogr. A* 837: 187–200.

Cheruiyot, N.K., Lee, W.J., Mwangi, J.K., Wang, L.C., Lin, N.H., Lin, Y.C., Cao, J.J., Zhang, R.J., Guo, P. and Chang, C. (2015). An overview: Polycyclic aromatic hydrocarbon emissions from the stationary and mobile sources and in the ambient air. *Aerosol Air Qual. Res.* 15: 2730–2762.

Crutzen, P.J. and Andreae, M.O. (1990). Biomass burning in the tropics: Impact on atmospheric chemistry and biogeochemical cycles. *Science* 250: 1669–1678.

Ferreiro, A., Merino, A., Díaz, N. and Piñeiro, J. (2011). Improving the effectiveness of wood-ash fertilization in mixed mountain pastures. *Grass Forage Sci.* 66: 337–350.

Fisher, T., Hajaligol, M., Waymack, B. and Kellogg, D. (2002). Pyrolysis behavior and kinetics of biomass derived materials. *J. Anal. Appl. Pyrolysis* 62: 331–349.

Hao, L., Zhu, L.Z. and Zhu, N.L. (2009). Polycyclic aromatic hydrocarbon emission from straw burning and the influence of combustion parameters. *Atmos. Environ.* 43: 978–983.

Kong, S.F., Shi, J.W., Lu, B., Qiu, W.G., Zhang, B.S., Peng, Y., Zhang, B.W. and Bai, Z.P. (2011). Characterization of PAHs within $PM_{10}$ fraction for ashes from coke production, iron smelt, heating station and power plant stacks in Liaoning Province, China. *Atmos. Environ*. 45: 3777–3785.

Košnář, Z., Mercl, F., Perná, I. and Tlustoš, P. (2016). Investigation of polycyclic aromatic hydrocarbon content in fly ash and bottom ash of biomass incineration plants in relation to the operating temperature and unburned carbon content. *Sci. Tot. Environ.* 563–564: 53–61.

Li, H., Liu, G.J. and Cao, Y. (2015). Levels and environmental impact of PAHs and trace element in fly ash from a miscellaneous solid waste by rotary kiln incinerator, China. *Nat. Hazards* 76: 811–822.

Li, Y.Y., Yang, L.X., Chen, X.F., Gao, Y., Jiang, P., Zhang, J.M., Yu, H. and Wang, W.X. (2017a). $PM_{2.5}$-bound PAHs in indoor and hotels in urban and suburban of Jinan, China: Concentrations, sources, and health risk impacts. *Aerosol Air Qual. Res*. 17: 2463–2473.

Li, Z.Y., Chen, L., Liu, S.T., Ma, H.Q., Wang, L., An, C.X. and Zhang, R.L. (2016). Characterization of PAHs and PCBs in fly ashes of eighteen coal-fired power plants. *Aerosol Air Qual. Res*. 16: 3175–3186.

Li, Z.Y., Ma, H.Q., Fan, L., Zhao, P., Wang, L., Jiang, Y.J., An, C.X., Liu, A.Q., Hu, Z.S. and Jin, H. (2017b). Size distribution of inorganic elements in bottom ashes from seven types of bio-fuels across Beijing-Tianjin-Hebei region, China. *Aerosol Air Qual. Res*. 17: 2450–2462.

Liu, J., Wang, Y., Li, P.H., Shou, Y.P., Li, T., Yang, M.M., Wang, L., Yue, J.J., Li, X.L. and Guo, L.Q. (2017). Polycyclic aromatic hydrocarbons (PAHs) at high mountain site in North China: Concentration, source and health risk assessment. *Aerosol Air Qual. Res*. 17: 2867–2877.

Liu, K.L., Xie, W., Zhao, Z.B., Pan, W.P. and Riley, J.T.

(2000). Investigation of polycyclic aromatic hydrocarbons in fly ash from fluidized bed combustion systems. *Environ. Sci. Technol.* 34: 2273–2279.

Liu, W.X., Dou, H., Wei, Z.C., Chang, B., Qiu, W.X., Liu, Y. and Tao, S. (2009). Emission characteristics of polycyclic aromatic hydrocarbons from combustion of different residential coals in North China. *Sci. Total Environ*. 407: 1436–1446.

Liu, X.J., Li, C.M., Tu, H., Wu, Y.Y., Ying, C., Huang, Q., Wu, S., Xie, Q.H., Yuan, Z.K. and Lu, Y.A. (2016). Analysis of the effect of meteorological factors on $PM_{2.5}$-associated PAHs during atumn-winter in urban Nanchang. *Aerosol Air Qual. Res*. 16: 3222–3229.

Lohmann, R., Northcott, G.L. and Jones, K.C. (2000). Assessing the contribution of diffuse domestic burning as a source of PCDD/Fs, PCBs, and PAHs to the UK atmosphere. *Environ. Sci. Technol.* 34: 2892–2899.

Mahua, S.H., Maharana, D., Kurumisawa, R., Takada, H., Yeo, B.G., Rodrigues, A.C., Bhattacharya, B., Kumata, H., Okuda, T., He, K.B., Ma, Y.L., Nakajima, F., Zakaria, M.P., Giang, D.H. and Viet, P.H. (2017). Seasonal trends of atmospheric PAHs in five Asian megacities and source detection using suitable biomarkers. *Aerosol Air Qual. Res*. 17: 2247–2262.

Masto, R.E., Sarkar, E., George, J., Jyoti, K., Dutta, P. and Ram, L.C. (2015). PAHs and potentially toxic elements in the fly ash and bed ash of biomass fired power plants. *Fuel Process. Technol.* 132: 139–152.

Nisbet, C. and LaGoy, P. (1992). Toxic equivalence factors (TEFs) for polycyclic aromatic hydrocarbons (PAHs). *Regul. Toxicol. Pharm.* 16: 290–300.

Orecchio, S. (2010a). Assessment of polycyclic aromatic hydrocarbons (PAHs) in soil of a natural reserve (Isola delle Femmine) (Italy) located in front of a plant for the production of Cement. *J. Hazard. Mater.* 173: 358–368.

Orecchio, S. (2010b). Analytical method, pattern and sources of polycyclic aromatic hydrocarbons (PAHs) in the stone of the temples of Agrigento (Italy). *J. Hazard. Mater.* 176: 339–347.

Orecchio, S. (2010c). Contamination from polycyclic aromatic hydrocarbons (PAHs) in the soil of a botanical garden localized next to a former manufacturing gas plant in Palermo (Italy). *J. Hazard. Mater.* 180: 590–601.

Orecchio, S., Amorello, D., Barreca, S. and Valenti, A. (2016a). Wood pellets for home heating can be considered environmentally friendly fuels? Polycyclic aromatic hydrocarbons (PAHs) in their ashes. *Microchemical* 124: 267–274.

Orecchio, S., Bianchini, F., Bonsignore, R., Blandino, P., Bareca, S. and Amorello, D. (2016b). Profiles and sources of PAHs in sediments from an open-pit mining area in the Peruvian Andes. *Polycyclic Aromat. Compd.* 36: 429–451.

Peng, N.N., Li, Y., Liu, Z.G., Liu, T.T. and Gai, C. (2016a). Emission, distribution and toxicity of polycyclic aromatic hydrocarbons (PAHs) during municipal solid waste (MSW) and coal co-combustion. *Sci. Tot. Environ.* 565: 1201–1207.

Peng, N.N., Liu, Z.G., Liu, T.T. and Gai, C. (2016b). Emissions of polycyclic aromatic hydrocarbons (PAHs) during hydrothermally treated municipal solid waste combustion for energy generation. *Appl. Energy* 184: 396–403.

Permadi, D.A. and Kim Oanh, N.T. (2013). Assessment of biomass open burning emissions in Indonesia and potential forcing impact. *Atmos. Environ.* 78: 250–258.

Ravindra, K., Sokhi, R. and Van Grieken, R. (2008). Atmospheric polycyclic aromatic hydrocarbons: Source attribution, emission factors and regulation. *Atmos. Environ*. 42: 2895–2921.

Singh, D.P., Gadi, R., Mandal, T.K., Saud, T., Saxena, M.A. and Sharma, S.K. (2013). Emission estimates of PAH from biomass fuels used in rural sector of indogangetic plains of India. *Atmos. Environ*. 68: 120–126.

Streets, D.G., Yarber, K.F., Woo, J.H. and Carmichael, G.R. (2003). Biomass burning in Asia: Annual and seasonal estimates and atmospheric emissions. *Global Biogeochem. Cycles* 17: 1099–1118.

Tobiszewski, M. and Namiésnik, J. (2012). PAH diagnostic ratios for the identification of pollution emission sources. *Environ. Pollut*. 162: 110–119.

Toscano, G., Duca, D., Amato, A. and Pizzi, A. (2014). Emission from realistic utilization of wood pellet stove. *Energy* 68: 644–650.

Tsai, J.H., Lin, K.H., Chen, C.Y., Ding, J.Y., Choa, C.G. and Chiang, H.L. (2007). Chemical constituents in particulate emission from an integrated iron and steel facility. *J. Hazard. Mater.* 147: 111–119.

Valavanidis, A., Iliopoulos, N., Gotsis, G. and Fiotakis, K. (2008). Persistent free radicals, heavy metals and PAHs generated in particulate soot emissions and residue ash from controlled combustion of common types of plastic. *J. Hazard. Mater.* 156: 277–284.

Wongphatarakul, V., Friedlander, S.K. and Pinto, J.P. (1998). A comparative study of $PM_{2.5}$ ambient aerosol chemical databases. *Environ. Sci. Technol*. 32: 3926–3934.

Yang, H.H., Lee, W.J., Chen, S.J. and Lai, S.O. (1998). PAH emission from various industrial stacks. *J. Hazard. Mater.* 60: 159–174.

Yang, H.H., Lai, S.O., Hsieh, L.T., Hsueh, H.J. and Chi, T.W. (2002). Profiles of PAH emission from steel and iron industries. *Chemosphere* 48: 1061–1074.

You, X.F., Li, X.D., Lu, S.Y., Jiang, N.M., Yan, J.H. and Cen, K.F. (2002). PAHs emission from co-combustion of MSW and coal. *J. Fuel Chem. Technol.* 30: 130–135. (in Chinese)

Zhang, Z.Z., Wang, W.X., Cheng, M.M., Liu, S.J., Xu, J., He, Y.J. and Meng, F. (2017). The contribution of residential coal combustion to $PM_{2.5}$ pollution over China's Beijing-Tianjin-Hebei region. *Atmos. Environ.* 159: 147–161.

Zhong, H., Xie, J., Yang, Z.T., Zhang, W.D. and Song, H.C. (2001). Biomass pyrolysis gasification technology research status and development. *J. Yunnan. Normal Univ.* 21: 41–45. (in Chinese)

Zhou, H.C., Jin, B.S., Xiao, R., Zhong, Z.P. and Huang, Y.J. (2009). Distribution of polycyclic aromatic hydrocarbons in

fly ash during coal and residual char combustion in a pressurized fluidized bed. *Energy Fuels* 23: 2031–2034.

*Received for review, December 21, 2017*
*Revised, February 12, 2018*
*Accepted, February 12, 2018*